


A reaction norm for flowering time plasticity reveals physiological footprints of maize adaptation

Justine Drouault,¹ Carine Palafre,² Emilie J. Millet,¹ Jonas Rodriguez,¹ Pierre Martre,¹ Kristian Johnson,¹ Boris Parent,¹ Claude Welcker,¹ Randall J. Wisser ^{1,3,*}

¹LEPSE, INRAE, L'Institut Agro, University of Montpellier, Montpellier 34060, FR

²Unité Expérimentale du Maïs, INRAE, Saint Martin De Hinx 40390, FR

³Department of Plant and Soil Sciences, University of Delaware, Newark, DE 19716, USA

*Corresponding author: Email: randall.wisser@inrae.fr

Understanding how plant phenotypes are shaped by their environments is crucial for addressing questions about crop adaptation to new environments. This study focused on analyzing genotype–environment interactions and adaptation for flowering time in maize. We present a physiological reaction norm for flowering time plasticity (PRN-FTP), modeled from multi-environment trial networks and decomposed into its physiological components. We show how genotype-specific differences in developmental responses to temperature fluctuations condition differences in photoperiod perceived among genotypes. This occurs not only across but also within common environments, as the perception of photoperiod is altered by variation in rates of development and durations for becoming sensitized to photoperiod. Using a new metric for envirotyping sensed photoperiods for maize, it was found that, at high latitudes, different genotypes in the same environment can experience up to hours-long differences in photoperiod. This emphasizes the importance of considering genotype-specific differences in the experienced environment when investigating plasticity. Modeling the PRN-FTP for globally representative breeding material showed that tropical and temperate germplasm occupy distinct territories of the trait space for PRN-FTP parameters. Placed in the historical context of maize, our findings suggest that the geographical spread and breeding of maize was mediated by a specific modality of ecophysiological adaptation of flowering time. Our study has implications for understanding crop adaptation and for future crop improvement efforts.

Keywords: adaptation; GxExM; envirotyping; flowering time; genomic prediction; maize

Introduction

Plants exhibit vast phenotypic diversity, the principal axis for adaptation and evolution. The classic formalism $P = G + E + G \times E$ describes how phenotypes are determined by combinations of genetic (G) and environmental (E) effects. Environmental effects result from varying external conditions that lead to distinct phenotypic outcomes for the same genotype, a phenomena known as plasticity (Bradshaw 1965). As 21st-century climate markedly shifts the environmental dimension to new frontiers, it is an important and opportune time to investigate plasticity and genetic variation in plastic responses ($G \times E$). For crop improvement, harnessing plastic responses to shifts in climate conditions can facilitate the adaptation of crops into new territories or to alternative cropping systems (Rising and Devineni 2020; Sloat et al. 2020; Zabel et al. 2021). Thus, approaches for modeling $G \times E$ that are rooted in the understanding of plasticity represent a promising direction for agricultural research (e.g. Millet et al. 2019; Cooper et al. 2020; van Voorn et al. 2023).

The functional relationship that defines a pattern of plasticity across an environmental gradient is known as a reaction norm, with parameters that quantify the direction and magnitude of phenotypic change (Roff 1997). The reaction norm provides a foundation for modeling phenotypic responses to the environment.

However, separate disciplines have conceived reaction norms in different ways. A common approach in quantitative genetics uses the Finlay–Wilkinson statistical model applied to multi-environment trials (METs) (Finlay and Wilkinson 1963), in which the phenotypic values of individual genotypes are regressed on an index defined by the mean values of all genotypes per environment. In this framework, phenotypes are typically for final characteristics measured at the whole-plant scale that are targets for selection, such as flowering time, plant height, or yield. This method has provided a convenient generalization for modeling reaction norms from METs where large collections of genotypes can be simultaneously tested across different environments, enabling a wide-scale analysis of $G \times E$ (e.g. Jarquín et al. 2014; Kusmec et al. 2017; Guo et al. 2023). Clearly, however, the environment is abstractly defined and is often confounded with latent environmental effects where mechanisms underlying $G \times E$ become elusive, resulting in a lack of biological interpretability. In contrast, focused on phenotyping of finer-scale traits in controlled settings, ecophysiologicals have characterized norms of reaction for physiological responses to specific environment variables, such as the nonlinear response of growth and development to temperature (Parent et al. 2010; Parent and Tardieu 2012). Embedding formalisms for such reaction norms in crop growth models allows an upscaling to the phenotypes for final characteristics. This is modeled as a function of

genotype-specific parameters and environmental conditions, with outcomes emerging from physiological mechanisms that dynamically regulate plant development in response to fluctuating conditions across time (Muller and Martre 2019). This approach provides biological perspective, but studying broad diversity of $G \times E$ is challenged by experimental constraints to measuring the parameters of physiological reaction norms. In our study, we hypothesized that parameterizing a physiological reaction norm from MET data would allow us to analyze the diversity of flowering time plasticity in maize (*Zea mays* subsp. *mays*) and provide unique insights into maize adaptation.

Physiological responses to multiple environmental factors modulate development which affects flowering time, particularly temperature and photoperiod (Simpson and Dean 2002; Colasanti and Coneva 2009; Blümel et al. 2015; Lee et al. 2021). The influence of temperature results in a speeding or slowing of development, while, for photoperiod sensitive genotypes, the influence of photoperiod results in the suppression of reproductive transition and a delay in flowering time (this occurs under long daylengths for short-day (SD) species and short daylengths for long-day (LD) species). The response to temperature occurs throughout a plant's life cycle, while the response to photoperiod is growth-stage specific. This is a crucial distinction for the work presented here. In maize, a facultative SD species, the stage at which plants become sensitized to photoperiod is not directly observable, but based on photoperiod-swap experiments has been found to occur immediately before tassel initiation (reproductive transition) if plants are grown specifically under SD conditions (Kiniry et al. 1983b; Bassiri et al. 1992). In SD conditions, tassel initiation is not repressed by photoperiod and temperature is the primary driver of development time and determinant for when a genotype reaches the sensitized stage. Above a critical photoperiod, under LD conditions, tassel initiation in photoperiod sensitive genotypes is delayed beyond the timing at which they reach their sensitized stage, with a time delay that depends on genotypic variation in the degree of photoperiod sensitivity in addition to temperature fluctuations during the period of delay. Thus, as physiological responses to temperature fluctuations across the development cycle interact with genotypic variation in rates of plant development and durations of the reproductive transition, different genotypes can reach the sensitized stage on different days, and therefore may perceive different photoperiods, even within the same environment. For photoperiod sensitive genotypes, the magnitude of response to photoperiod is an additional source of plasticity that varies genetically, culminating in the formation of $G \times E$ interactions in flowering time across environments. We introduce these first-principles expectations for $G \times E$ interactions in flowering time, but we are not aware of studies that have thoroughly considered this in the construction of reaction norms from MET data.

The timing of reproductive transition (and consequently flowering) is controlled by a genetic regulatory network (GRN) that integrates both exogenous and endogenous signals (Song et al. 2015). A reference topology of this GRN in maize consists of multiple pathways including the circadian clock, photoperiod, autonomous, aging, and gibberellic acid pathways (Dong et al. 2012). However, the complete topology and context-dependent expression of the GRN is far from being fully understood (Minow et al. 2018; Stephenson et al. 2019). A key distinction exists in the way the GRN functions between LD and SD environments, with daylength-dependent and daylength-independent responses for photoperiod sensitive and insensitive genotypes. For example, the circadian clock pathway plays a central role in the transduction of signals to the other pathways, with a direct link between

external light conditions and the photoperiod pathway (in both LD plants like *Arabidopsis*—Sawa et al. 2007; Sawa and Kay 2011; and SD plants like maize—Bendix et al. 2013). Under LD conditions, transduction of light perception by the circadian clock to the photoperiod pathway represses production of the FT-derived florigen signal for reproductive transition in photoperiod sensitive genotypes of maize—flowering time is delayed (Meng et al. 2011). In contrast, the mechanism controlling floral transition is configured differently in insensitive genotypes of maize, with recent research implicating separate clock components that interact with the autonomous pathway (Minow et al. 2018). Less is known about the determination of critical thresholds for photoperiod sensitivity. A gating mechanism involving the circadian clock and photoperiod pathways has been described in rice (Itoh et al. 2010; Nemoto et al. 2016), with additional findings suggesting a conditional link involving the autonomous pathway described in maize (Matsubara et al. 2008; Park et al. 2008). While molecular genetic studies continue to elucidate the intricate dynamics of cross-talk and signal transduction by the GRN, a challenge is to relate this to functional diversity at the whole plant level. Thus, new approaches to characterizing the wider scale variation in ecophysiological plasticity for flowering time are needed.

This study focused on the modeling and analysis of a physiological reaction norm for flowering time plasticity (PRN-FTP) that integrates genotype-specific sensing and responses in growth and development to fluctuating temperatures and photoperiods, ultimately resulting in $G \times E$ for flowering time. Building on previous work (Kiniry et al. 1983a; Choquette et al. 2023), the PRN-FTP was formulated as a bilinear, threshold-dependent function that relates thermal time from crop emergence to flowering with a novel envirotyping index for the daylength sensed (DL^s) by individual genotypes in each environment. We envirotyped DL^s across field environments in the Northern Hemisphere to understand how photoperiod perception varies among genotypes both within and across environments, and whether genotype-specific values for DL^s should be used for modeling the PRN-FTP. We further demonstrate how analyzing the PRN-FTP as a bilinear function allows the decoupling of different components of flowering time variation: (i) flowering time *per se*; (ii) critical photoperiod; and (iii) photoperiod sensitivity; with genotype-specific parameter values estimated from MET data.

Finally, PRN-FTP parameters may be used to understand how flowering time plasticity varies among population groups or mediates adaptation to novel environments, and how this in turn alters flowering time plasticity for the future. Historical varieties of maize that spread from their tropical origins into temperate zones required adaptations to cooler climates with longer photoperiods, with studies implicating the central role of flowering time (Tenaillon and Charcosset 2011). For instance, several flowering time genes in the GRN for flowering time have been linked to the postdomestication spread of maize (e.g. *Vgt1*—Ducrocq et al. 2008; *ZmCCT10*—Hung et al. 2012; Yang et al. 2013; *ZCN8*—Guo et al. 2018; *ZmELF3.1*—Zhao et al. 2023). Here, we show that the trait space for the PRN-FTP parameters flowering time *per se* and photoperiod sensitivity putatively reflects how adaptation and selection history has shaped differences in flowering time plasticity between breeding pools of modern maize.

Materials and methods

A general guide to the study design and use of datasets 2–4 is presented in Fig. 1.

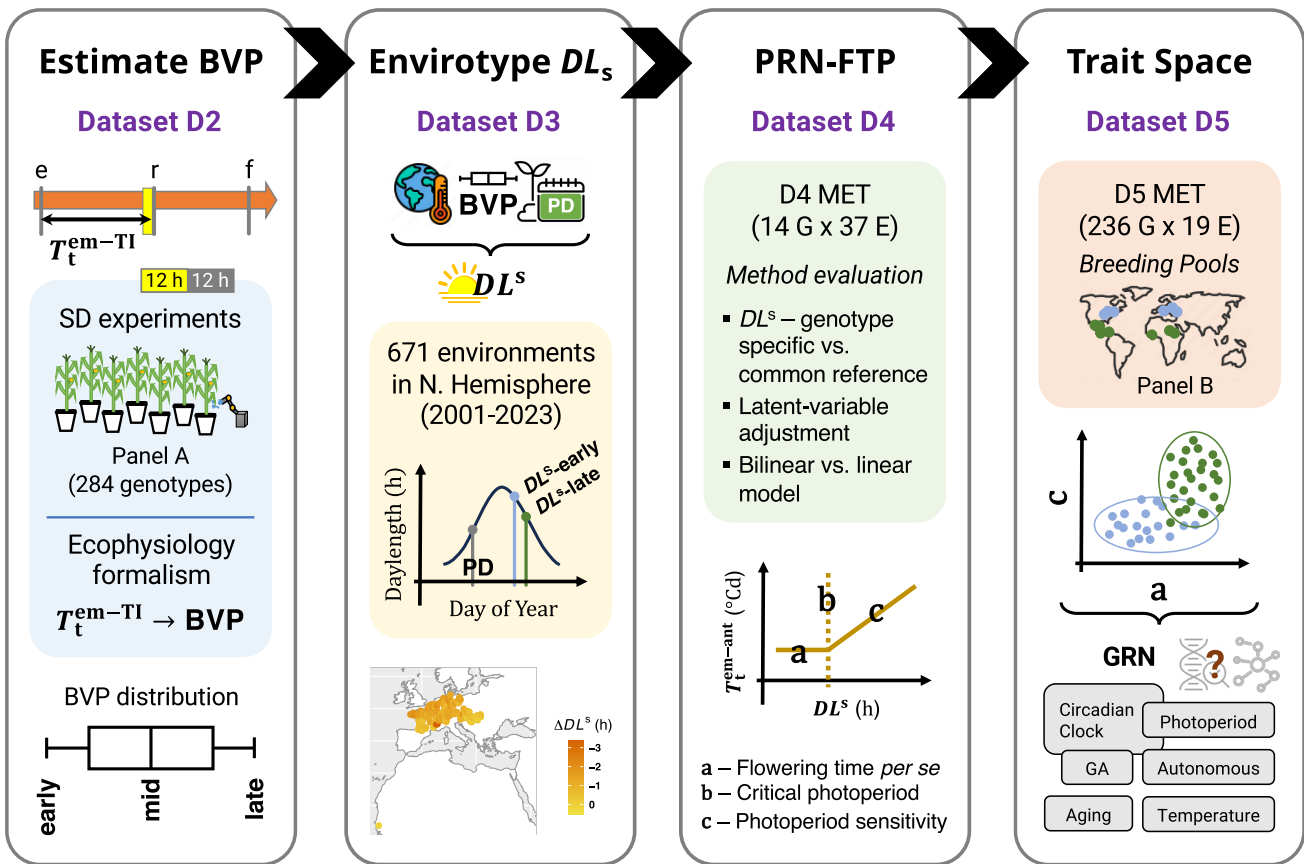


Fig. 1. Graphical guide to the study. Each panel portrays the main parts of the study performed with datasets 2–4 (dataset 1 was used to evaluate the choice of a temperature response function for calculating thermal time, not shown): (i) The estimation of basic vegetative phase (BVP) follows from prior research showing that the photoperiod-sensitized stage is reached just prior to the thermal-time required for reproductive transition (T_t^{em-TI}) for plants grown under SD conditions. This is depicted by the arrow marked with the timing of emergence (“e”), reproductive transition (“r”), and flowering (“f”). The full orange shading of the arrow represents that plants sense temperature throughout their life cycle, while the yellow-filled box preceeding the reproductive transition represents that photoperiod begins to be sensed at a particular stage of the life cycle. Data from SD experiments were used to estimate the BVP distribution for genotype-panel A ($n = 284$ genotypes). (ii) The temperature data from maize fields, BVP reference values for early, mid, and late maturing genotypes, and planting dates (“PD”) were used to envirotype the daylength sensed (DL_s) by each maturity class in 671 environments. The figure in the shaded region depicts how DL_s can vary between early and late maturing genotypes that become sensitized to photoperiod on different days of the year (this can vary due to fluctuations in temperature and rates of photoperiodic change). This was used to characterize inter- and intraenvironmental variation in DL_s for maize in the Northern Hemisphere. (iii) The physiological reaction norm for flowering time plasticity (PRN-FTP) was modeled using MET data on 14 genotypes in 37 environments. An evaluation of the methodologies for modeling the PRN-FTP was performed as noted in the shaded area. The figure portrays the PRN-FTP modeled as a bilinear function with coefficient estimates for flowering time *per se* (a, units °C), critical photoperiod (b, units h), and photoperiod sensitivity (c, units °Ch⁻¹). (iv) The PRN-FTP was modeled as a linear function (LD–SD method, see text) using MET data for genotype-panel B ($n = 236$ genotypes) in 19 environments. The trait space defined by flowering time *per se* (a) and photoperiod sensitivity (c) was used to infer about historical adaptation in maize. The map in the shaded area portrays genotypes from temperate (blue) and tropical (green) breeding pools of maize comprising genotype-panel B. The trait-space plot reflects a finding of this study, showing that tropical and temperate breeds occupy different territories of the space. Future research on the genetic dissection of the separate parameters may be used to relate ecophysiological scale variation to pathways in the gene regulator network (GRN) for reproductive transition and flowering time.

Datasets

Summarized in [Supplementary Table S1](#), datasets (“D”) from multiple projects and experiments on maize were assembled to: (D1) select a temperature response function for thermal time estimation; (D2) estimate variation in the thermal time duration between crop emergence and tassel initiation (T_t^{em-TI}) in order to develop a predictor function for indexing sensed photoperiod (DL_s); (D3) envirotype DL_s for diverse genotypes in maize fields across the Northern Hemisphere; (D4) demonstrate methods for modeling a physiological reaction norm for flowering time plasticity (PRN-FTP); and (D5) compare the trait space of parameters estimated from the PRN-FTP in a diversity panel constituting separate breeding pools of maize. A brief description of the datasets used

for these five objectives are presented first, followed by methods and other details in subsequent sections. The current study focused on days to anthesis (male flowering) as the final characteristic.

(D1) This dataset contains 24 hybrid genotypes measured for days to anthesis in 25 to 26 field experiments, spanning latitudes from 30.5371°N to 44.2089°N ([Supplementary File S1](#)). For each environment, the sowing date, field coordinates, and best linear unbiased estimates (BLUEs) for calendar days from sowing to anthesis were obtained from [McFarland et al. \(2020\)](#) and [Rogers et al. \(2021\)](#).

(D2) This dataset contains a collection of 284 inbred genotypes (panel A) with trait data combined from two experiments.

Emergence time and phyllochron were measured under well-watered conditions in a greenhouse phenotyping platform at the LEPSE of INRAE (PhenoArch, Montpellier, FR; [Cabrera-Bosquet et al. 2016](#)). Final leaf number was measured under well-watered conditions in a field environment in Puerto Vallarta, MX. Both experiments were performed under SD conditions, where day-lengths throughout the growth cycle never exceeded 12.5 h. Further details for these experiments and the estimation of genotypic effects can be found in [Supplementary Information \(Methods S2\)](#).

(D3) This dataset contains the geographical coordinates and planting dates for 671 field environments across the Northern Hemisphere (latitudinal range of 13.7578°N to 54.2900°N) assembled from previous and new projects ([Supplementary File S3](#)).

(D4) This dataset contains a collection of seven temperate inbred genotypes (B37, B73, M37W, Mo17, Oh43, LH123Ht, and 2,369) and seven tropical inbred genotypes (CML10, CML258, CML277, CML341, CML373, Tzi8, and Tzi9) measured for days to anthesis in 37 field experiments ([Supplementary File S4](#)). Assembled from previous and new projects, it represents a multi-environment trial (MET) dataset designed to maximize the presence of these 14 genotypes, which were also included in dataset D2. However, their representation across environments was uneven, with temperate genotypes tested in 15 to 22 environments and tropical genotypes in 18 to 37 environments.

(D5) This dataset contains a collection of 109 temperate, 66 tropical, and 61 admixed inbred genotypes, representing separate breeding pools (panel B; [Liu et al. 2003](#); [Flint-Garcia et al. 2005](#)), measured for days to anthesis across an MET with a maximum of 19 field experiments ([Supplementary File S5](#)). It was assembled from previous projects with an imbalanced representation of photoperiod conditions, including a maximum of three SD environments (maximum photoperiod <12.4 h) and 16 LD environments (minimum photoperiod >14.5 h), spanning latitudes from 18.00°N to 42.76°N.

Environmental data

For field environments considered in this study, temperature data were acquired from ground and satellite data sources for a common reference point of 2 m height. Ground data were obtained mostly from weather stations at a given field location. In two cases, ground data from a nearby airport within 5 km of the experimental field site was obtained from Weather Underground (<https://www.wunderground.com/>). Satellite data (weather variable “T2M”; spatial resolution of $\frac{1}{2}^\circ$ latitude \times $\frac{5}{8}^\circ$ longitude) was acquired from the R package *nasapower* ([Sparks 2018](#)) using the latitude and longitude coordinates for each field location.

The photoperiod based on civil twilight at a given location for a given day of the year was acquired from the R package *TrenchR* ([Buckley et al. 2023](#)). This uses the CBM daylength model described by [Forsythe et al. \(1995\)](#).

Comparison of temperature response functions

Throughout this study, calendar days were converted into thermal time to account for growth and development variations caused by temperature differences across field environments. We evaluated three temperature response functions for calculating thermal time using dataset D1 ([Supplementary Methods S1, equations S1–S3](#)). This comparison was based on the assumption that temperature-driven growth and development primarily determine the time to flowering in photoperiod-insensitive genotypes. Under this assumption, temperature differences alone should explain most of the variation in days to anthesis across

environments. The function that produces the most consistent thermal time to anthesis values for a given genotype across environments would, therefore, be considered the best. Dataset D1 was used for this assessment since it consisted of temperate-adapted maize hybrids (generally known to be photoperiod insensitive) tested across many independent field environments.

For each of the 24 hybrids, BLUEs for days to anthesis from each field experiment were converted into thermal time using each function. Then, the normalized root mean square error (NRMSE, normalized by the difference between maximum and minimum values) of function-specific thermal times was computed for each genotype. The results were compared to identify the function that minimized the NRMSEs overall. For the purpose of comparing different models for thermal time estimation with the same dataset, we assumed the influence of any latent variables on growth and development could be ignored.

Definition of a physiological reaction norm for flowering time

The PRN-FTP was reformulated from a previous model by [Kiniry et al. \(1983a\)](#) that described the relationship between photoperiod (x-axis) and thermal time from crop emergence to tassel initiation ($T_t^{\text{em-TI}}$) based on temporal dissections of shoot apical meristems (y-axis). [Kiniry et al. \(1983a\)](#) used growth chambers in which constant levels of photoperiod were applied throughout the plant's growth cycle, so DL^s had a known value in each treatment. However, in field environments photoperiods are not constant (DL^s depends on the day of year within a given environment when a plant becomes sensitized to photoperiod), and estimating tassel initiation from dissections of meristems is not practical at large scale (rather, in METs, days to flowering are routinely recorded). Besides, as described in the introduction, even direct observation of tassel initiation does not correspond to the timing when photoperiod-sensitive genotypes become sensitized to photoperiod in LD environments. Therefore, we devised an approach for predicting this unobservable stage of photoperiod sensitization, such that DL^s could be determined for a given genotype in a given environment. Thus, adapted for METs that cover SD and LD environments, this study defined the PRN-FTP as the relationship between a new proxy measure for DL^s (x-axis) and thermal time from crop emergence to anthesis ($T_t^{\text{em-ant}}$; y-axis).

Procedure for DL^s estimation (x-axis of the PRN-FTP)

There are two main steps used for determining DL^s . First, the $T_t^{\text{em-TI}}$ is estimated for genotypes grown under SD conditions in which a photoperiod response is not triggered. In this study, an ecophysiological formalism was used to predict $T_t^{\text{em-TI}}$ ([equation 1](#)) from experimental data. This is expected to closely approximate the amount of thermal time it takes for a given genotype to become sensitized to photoperiod, which has been referred to as the basic vegetative phase (BVP; [Kiniry et al. 1983b](#)). Second, the calendar day on which the total thermal time for the BVP is reached is determined using temperature records for a given environment. The daylength for that specific day is then obtained for DL^s . As applied in this study, the two steps of this procedure are as follows:

Step 1: An ecophysiological formalism ([equation 1](#)) was used to estimate BVP for the 284 genotypes in panel A that were phenotyped in SD experiments (dataset D2; [Supplementary Methods S2](#)). Therefore, even though the panel included photoperiod sensitive genotypes, their photoperiod responses were not triggered, such that estimates of $T_t^{\text{em-TI}}$ correspond to the BVP. Considering that tassel initiation occurs on the day when the last leaf

primordium is formed (Lejeune and Bernier 1996) and that rates of leaf primordia formation and leaf tip appearance are proportional (Padilla and Otegui 2005), $T_t^{\text{em-TI}}$ can be calculated as:

$$T_t^{\text{em-TI}} = \frac{P_{\text{tip}_i}}{\alpha_{\text{phyll/plast}}} (L_{F_i} - L_{\text{pri}}^{\text{em}}), \quad (1)$$

where, $T_t^{\text{em-TI}}$ ($^{\circ}\text{Cd}$) is the cumulative thermal time from crop emergence to tassel initiation of the i th genotype, P_{tip_i} (leaf $^{\circ}\text{Cd}^{-1}$) is the phyllochron of the i th genotype (i.e. the thermal time between the appearance of two successive leaf tips), L_{F_i} (leaf) is the final leaf number of the i th genotype, $\alpha_{\text{phyll/plast}}$ (dimensionless) is a constant ratio of phyllochron to plastochron (i.e. the thermal time between the formation of two successive leaf primordia), and $L_{\text{pri}}^{\text{em}}$ (primordium) is a constant number of primordia formed at crop emergence. Genotype-specific values for P_{tip_i} and L_{F_i} were estimated for panel A (dataset D2; [Supplementary Methods S2](#)). For maize, $\alpha_{\text{phyll/plast}}$ may range from 1.58 to 1.85 (Kiniry 1991; Lejeune and Bernier 1996; Padilla and Otegui 2005; Andrieu et al. 2006). In this study, we set it at the average value reported in the literature (1.73). There are four to five leaf primordia in the embryo of maize seeds (Bonnett 1954; Padilla and Otegui 2005), and between germination and crop emergence about two other leaf primordia are formed (Padilla and Otegui 2005). Thus, here, $L_{\text{pri}}^{\text{em}}$ was set equal to 5.5 primordia.

Step 2: Using $T_t^{\text{em-TI}}$ the BVP of a given genotype, along with emergence date and temperature records from a given environment, the calendar day on which the genotype becomes sensitized to photoperiod was predicted. When observed emergence dates were unavailable, a thermal time of 76°Cd was assumed for the period from sowing to emergence. This was estimated from observed data for 15 environments within dataset D4 (sourced from the Maize ATLAS project; see [Supplementary Table S1](#)), calculated using the temperature response function [Supplementary equation S2](#).

Thermal time from crop emergence to anthesis (y-axis of the PRN-FTP)

For each genotype in each environment, $T_t^{\text{em-ant}}$ was calculated as the cumulative thermal time between the dates of emergence date (observed or predicted) and anthesis (determined from BLUEs of days to anthesis).

Envirotyping of sensed photoperiod

Dataset D3 was used to computationally envirotype DL^s across 671 environments in the Northern Hemisphere. In each environment, DL^s was envirotyped for three maturity levels defined by the lower (5th; early maturity), median (50th), and upper (95th; late maturity) percentiles of the BVP distribution estimated for panel A (dataset D2; [Table 1](#)). The difference in DL^s between maturity levels was calculated to assess how genotypes with different BVPs may vary in the photoperiod they perceive within a given environment. Knowing that daily changes in photoperiod increase with latitude, the per-environment differences in DL^s were compared to rates of photoperiodic change. The rate of photoperiodic change within

each environment was calculated from photoperiods between the days immediately before and immediately after DL^s for the 50th-percentile maturity level. When modeling the PRN-FTP for each genotype from MET data, $T_t^{\text{em-ant}}$ (response variable) values will correspond to the environment-specific observations for each genotype, while DL^s (predictor variable) could either be based on the BVP for the same particular genotype or a common reference representing all genotypes. The choice depends first on whether BVP data are available for all genotypes in the MET, but also whether different genotypes in the same environment experience large or small differences in photoperiod.

Statistical analysis of the PRN-FTP

Two different regression functions, bilinear and linear, were used for modeling the PRN-FTP. This involved two different approaches as follows:

Bilinear function for estimating three parameters of the PRN-FTP. With a sufficient density of data and coverage of DL^s spanning SD and LD environments, photoperiod sensitive genotypes are expected to follow a bilinear pattern of response. That is, in SD environments $T_t^{\text{em-ant}}$ remains relatively constant, and above a critical threshold for LD environments it increases linearly with photoperiod. For this type of response, the PRN-FTP can be modeled as a continuous two-phase (bilinear) regression function with threshold detection (Fong et al. 2017a). We used the “hinge model” in the R package *chnp* (Fong et al. 2017b), defined as follows:

$$T_t^{\text{em-ant}} = \alpha + \beta(DL^s - e)_+, \quad (2)$$

where $T_t^{\text{em-ant}}$ (described before) is the response variable; e is the threshold parameter; DL^s is the sensed daylength with a threshold effect; $I(DL^s > e) = 1$ when $DL^s > e$ and 0 if $DL^s \leq e$; $(DL^s - e)_+$ denotes the hinge function, which equals $DL^s - e$ for $DL^s > e$ and 0 otherwise; and α and β are the intercept and slope parameters, respectively. The model was fitted using default settings for *chnp*, with no constraints set for estimating the threshold value (breaking point of the bilinear model). Estimated effects include an intercept, threshold value, and slope, which correspond to physiological components of flowering time: the flowering time *per se*, a critical threshold for photoperiod sensitivity, and the degree of photoperiod sensitivity, respectively.

Linear function for estimating two parameters of the PRN-FTP. When fitting the bilinear model is not feasible due to insufficient density of data, inadequate coverage of DL^s for threshold detection, or because it is not an appropriate model for all genotypes (i.e. photoperiod insensitive genotypes), we modeled the PRN-FTP as a linear regression function, forgoing threshold estimation. So that the intercept for $T_t^{\text{em-ant}}$ is estimated at the mean DL^s of SD environments rather than the shortest day environment, environments across the MET were first classified as SD or LD based on whether DL^s falls below or above a fixed threshold, respectively (we used 13.5 h which corresponded to the average threshold estimated from the analysis of dataset D4, see Results). The predictor values for each environment were then recoded as the mean DL^s value for the respective SD and LD environments in the regression model. Finally, when specifying the linear regression model, the SD and LD DL^s means are offset with the mean SD- DL^s value set to zero to obtain the proper intercept estimate for the corresponding genotype. Hereafter, we refer to this as the “LD-SD” method for modeling the PRN-FTP. This is similar to prior studies that used the difference between mean thermal times to flowering in LD and SD environments as an estimate of photoperiod sensitivity

Table 1. Distribution percentiles for the basic vegetative phase and leaf tip appearance at tassel initiation of panel A.

	Min	5%	25%	50%	75%	95%	Max
BVP-ti ($^{\circ}\text{Cd}$)	169	239	286	326	375	434	496

(Coles et al. 2010; Hung et al. 2012), except here an intercept for flowering time *per se* (in units °C) and slope for photoperiod sensitivity (in units °Ch⁻¹) are estimated.

N.B.—Two particular points are relevant for interpreting parameters estimated by the LD–SD method. First, envirotyping of DL^s to obtain the mean values for SD and LD environments may be based on each specific genotype being modeled or a common reference genotype (this point is described in other parts of the study). Even if a common reference BVP is used to envirotype DL^s for all genotypes, the mean values for DL^s can vary due to imbalanced observations of the genotypes across environments, which occurs frequently in MET data. That is, although DL^s may be envirotyped for a common reference BVP in each environment, the regression analysis is performed using predictor values linked to the observed $T_{\text{crit}}^{\text{em-ant}}$ data being modeled for each genotype. Second, for photoperiod sensitive genotypes, it is expected that estimates of photoperiod sensitivity will be biased as a function of the deviation between the SD– DL^s value and the true (unknown) critical photoperiod for a given genotype. When the true critical photoperiod is less than the SD– DL^s value, the estimate will be upward biased, and when it is greater it will be downward biased.

Correction for latent variables affecting thermal times to anthesis. If only temperature influenced the flowering time of a photoperiod insensitive genotype, we expect its $T_{\text{crit}}^{\text{em-ant}}$ would be nearly identical across all environments in an MET. However, aside from photoperiod sensitivity, misrepresentation in the temperature response function, or measurement error, deviations in $T_{\text{crit}}^{\text{em-ant}}$ could be due to several other possibilities that vary from one environment to another, including the influence of other environmental factors, differences in crop management practices, differences between air temperature and the temperature sensed by the crop, imprecision and biases in weather data, or other latent variables. Therefore, with dataset D4, we tested an alternative approach using photoperiod insensitive control genotypes to adjust for the effects of latent variables across environments prior to constructing the PRN-FTP.

Seven photoperiod insensitive genotypes were defined as control genotypes in dataset D4. The 37 environments comprising the MET were assembled from different experiments. Unfortunately, all seven control genotypes were not present in all environments, so two sets of control groups were defined (set 1: B37, B73, M37W, Mo17, and Oh43; set 2: LH123Ht and 2,369). Sets 1 and 2 were associated with 22 and 15 of the environments, respectively. For each set, the overall mean of $T_{\text{crit}}^{\text{em-ant}}$ was calculated across environments of the MET in which they were present. The environment-specific residuals were then used to adjust the thermal times for the remaining noncontrol genotypes in each corresponding environment. We note that using two sets of control genotypes that were also imbalanced across environments (see the earlier description of dataset D4) is not ideal and could introduce some bias, but any improvement in the model fit would presumably reflect positively on this approach. Therefore, using dataset D4, we compared the overall RMSE of the PRN-FTP model fit and standard errors of parameter estimates before and after applying the correction method.

Applications of the PRN-FTP

Datasets D4 and D5 were used to test the concepts developed in this study for modeling and analyzing the PRN-FTP from MET data.

Methodological evaluation

The MET for dataset D4 had a sufficient coverage of DL^s for fitting the bilinear model (assumed to be the biologically correct one).

Additionally, BVP values from dataset D2 could be used to obtain genotype-specific DL^s values for the genotypes in D4. This allowed us to test different approaches to modeling the PRN-FTP, including: (i) the impact of using latent-variable adjusted values of $T_{\text{crit}}^{\text{em-ant}}$; (ii) the impact of envirotyping DL^s using genotype-specific values vs a common reference value for the BVP; and (iii) the impact of using the bilinear model vs the LD–SD method on the estimated parameters for flowering time *per se* and photoperiod sensitivity (the threshold for critical photoperiod can only be estimated with the bilinear model). Although this was performed with only seven tropical maize genotypes, analysis with the bilinear model also provided a preliminary survey of potential variation in the three PRN-FTP parameters for maize.

Analysis of maize diversity

We sought to investigate the wider variation in PRN-FTP parameters in a diverse collection of 236 maize genotypes adapted to different geographical zones (dataset D5). However, due to both an insufficient density and coverage of DL^s and the mixed composition of photoperiod sensitive and insensitive genotypes, the bilinear function could not be fit. This was true even for genotypes known to be photoperiod sensitive, such as those used for methodological evaluation (we observed bogus estimates of the parameters). Moreover, most of the genotypes were not present in dataset D2 so genotype-specific BVP values for DL^s envirotyping could not be systematically used. Therefore, for dataset D5, the LD–SD method was applied, with DL^s values obtained using the BVP for the 50th-percentile reference maturity determined with dataset D2 (Table 1). The regression model was fit using latent-variable adjusted BLUEs for $T_{\text{crit}}^{\text{em-ant}}$ regressed onto mean DL^s for the SD and LD environments as described in the previous section. Latent variable adjustment was performed using the set 1 control group (indicated above) common across the dataset D5 MET.

Results

Choosing a temperature response function to construct the PRN-FTP

Thermal time is used to determine DL^s for envirotyping along with $T_{\text{crit}}^{\text{em-ant}}$ for modeling the PRN-FTP, such that different temperature response functions for calculating thermal time could result in different outcomes. A comparison of three different temperature response functions showed no significant difference in the NRMSEs for thermal times to anthesis for 24 photoperiod-insensitive hybrids tested in 25 to 26 environments in North America. Regardless of the temperature response function that was tested, for each hybrid, the environment-specific thermal time to anthesis deviated, on average, by 10% (range 9 to 13%) from the across-environment mean (Supplementary Fig. S1). Therefore, for the current study, we chose the nonlinear response function by Wang and Engel (1998) adapted for maize (Supplementary equation S2) due to its common implementation in crop growth models (Wang et al. 2017), its higher physiological realism compared with the linear response function (Supplementary equation S1), and its greater flexibility compared to the Arrhenus model (Parent et al. 2010).

Predicting when maize becomes sensitized to photoperiod

There is no known visible marker to measure the timing when maize plants become sensitized to photoperiod for determining DL^s . Therefore, we defined this using the BVP ($T_{\text{crit}}^{\text{em-TI}}$ in SD conditions), which closely corresponds to the thermal time required

for plants to reach their photoperiod-sensitized stage (Kiniry *et al.* 1983b; Bassiri *et al.* 1992). An issue is that directly observing tassel initiation requires temporal dissections of shoot apical meristems which is not possible at a large scale. To circumvent this, we used an ecophysiological formalism to estimate $T_t^{\text{em-TI}}$ (equation 1) for the 284 genotypes in panel A grown under SD conditions (dataset D2; Supplementary File S2). A separate SD experiment validated this for eight of the genotypes using microscopy data on differentiation of shoot apical meristems into tassel primordia (Supplementary Methods S2). The Pearson correlation coefficient between predicted and observed BVP values was 0.84, indicating the formalism-based predictions for $T_t^{\text{em-TI}}$ align closely with observational data. Table 1 summarizes percentiles of the BVP distribution for panel A, with the 5th, 50th, and 95th percentile values used to represent early, medium, and late maturity groups for envirotyping DL^s .

Spatiotemporal variation in the sensed photoperiod for maize

Envirotyping with DL^s can be used to understand how different genotypes sense photoperiod across and within environments, and how this varies according to spatiotemporal patterns in climate and weather. To examine how photoperiods are perceived by maize, we computationally envirotyped DL^s for 671 field environments across the Northern Hemisphere where maize has been previously grown (Fig. 2).

We first summarized the spatial axis of variation in DL^s using the 50th percentile of $T_t^{\text{em-TI}}$ (326°Cd) as a common reference for envirotyping (Table 1; Supplementary Fig. S2). The range in DL^s across the entire set of environments evaluated was 11.9 to 18.3 h, a difference of 6.4 h (Fig. 2a). We compared the DL^s for maize above 30°N in the USA and Europe, corresponding to regions where maize is used extensively for scientific research and agricultural production (Fig. 2a, b). Mean DL^s across the USA was 16.2 h and in Europe was 16.7 h, with lower (5-percentile) to upper (95-percentile) ranges of 14.3 to 16.4 and 15.7 to 17.5, respectively. These spatial patterns are primarily driven by climatic variation in photoperiod across latitude coupled with the seasonality for maize cultivation. Since temperature can speed or slow growth and development, interannual differences in temperature and planting dates at the same location can give rise to additional variation in DL^s for maize. To examine this, we selected 118 field sites where maize was planted for at least 2 years and found that DL^s within a single location varied by as much as 1.7 h, with a mean absolute difference of 0.3 h.

Next, we questioned the extent to which multiple genotypes grown within the same field environment perceive a different photoperiod. Beyond the equator, photoperiod is not constant across days of the year, with increasing rates of daily change in association with latitude. Therefore, genotypes differing in BVP that reach their photoperiod-sensitized stage on different days would perceive a different photoperiod (Fig. 2b, c), but to our knowledge the magnitude by which this varies has not been investigated.

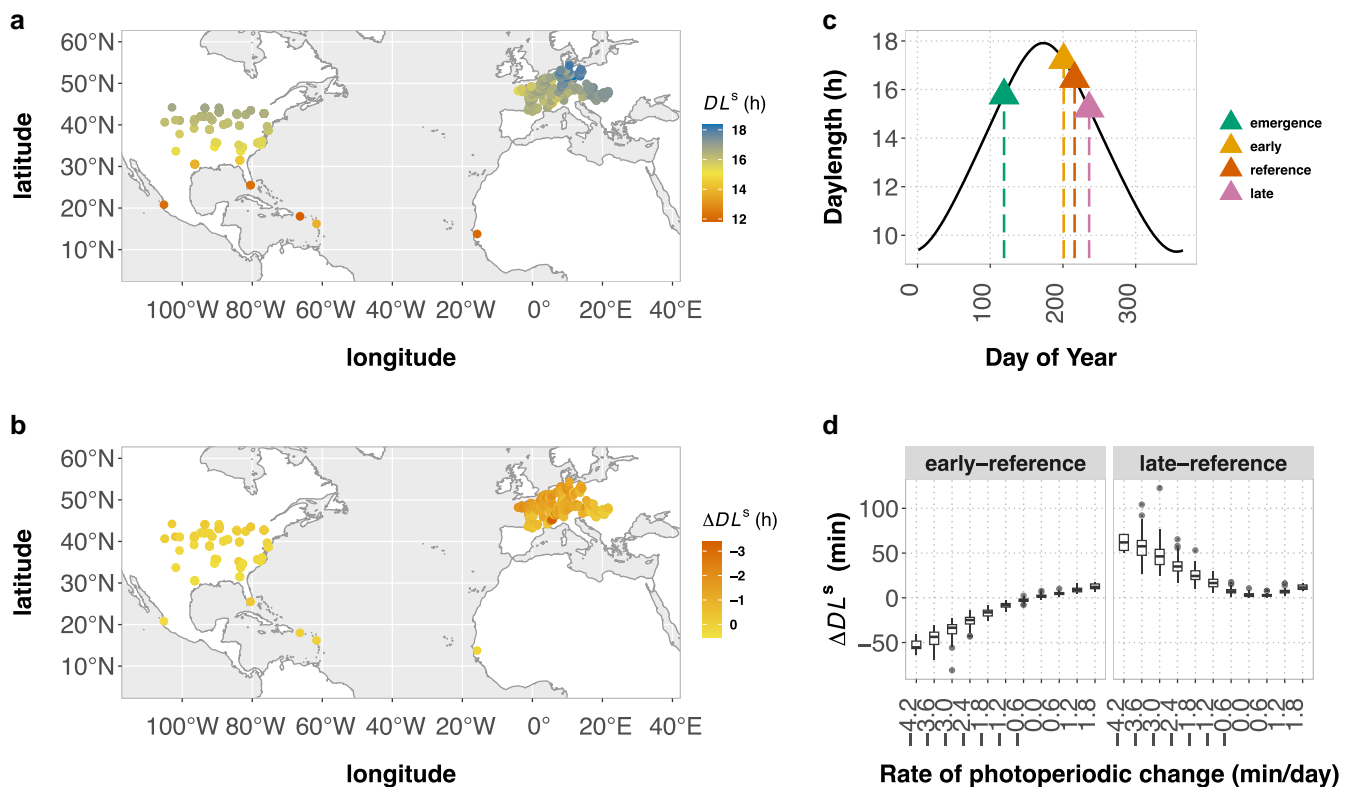


Fig. 2. Envirotyping of sensed photoperiod across and within maize fields in the Northern Hemisphere. a) Sensed photoperiod (DL^s for the 50th-percentile maturity reference) across maize field sites in the Northern Hemisphere. b) Within environment differences in hours of sensed daylength (DL^s) between the 95th and 5th percentile maturity groups defined by the BVP distribution of genotype-panel A. c) The figure portrays an example of one environment in which the photoperiod sensitized stage is reached on different days of the year for early (5th percentile), reference (50th percentile), and late (95th percentile) maturity levels, leading to differences DL^s . d) The relationship between within environment differences in DL^s and rates of daily photoperiodic change. Here, the differences are shown in minutes for comparisons between the reference maturity group relative to the early and late maturity groups. As reflected in b), the boxplots show that genotypes within the same environment experience increasingly greater differences in photoperiods when rates of photoperiodic change increase, which occurs in association with increasing latitude.

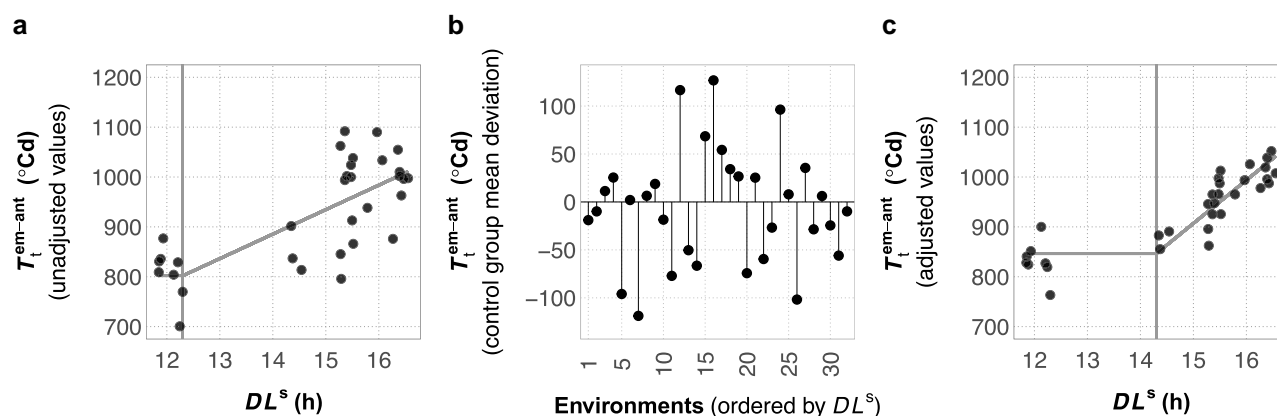


Fig. 3. Adjusting for latent variable effects across an MET network when fitting the PRN-FTP. a) The PRN-FTP for genotype CML341 based on unadjusted BLUEs for thermal time from crop emergence to anthesis (T_t^{em-ant} ; black points). Gray lines show the estimated flowering time *per se* (horizontal line), critical threshold value (vertical line), and photoperiod sensitivity (sloped line). b) Deviations from the overall average T_t^{em-ant} for the control groups of photoperiod insensitive genotypes estimated across the same environments. This is shown for the same 32 of 37 environments in dataset D4 where BLUEs were available for CML341. The datapoints are ordered along the x-axis (environment identifiers 1–32) in corespondence with plots a) and c) according to sensed daylength (DL^s). c) The PRN-FTP for genotype CML341 after adjusting the BLUEs by deviations in b), leading to different estimates for the flowering time *per se*, the critical threshold value, and the photoperiod sensitivity.

Using the 5th (239°Cd) and 95th (434°Cd) percentiles of the BVP distribution (Table 1) to represent early and late percentile-maturity groups, the DL^s at these limits frequently differed by more than 1 h, with the largest difference reaching 3.8 h (Fig. 2b). Differences in DL^s above 2 h were rare and occurred only in locations at high latitudes where late genotypes are not cultivated for maize production. Nevertheless, this highlights how the genetic diversity of maize can intersect with environmental variation within the same field, leading to differences in the photoperiod to which genotypes respond.

If the 50th-percentile for BVP is used as a common reference for envirotyping DL^s , the magnitude of inaccuracy compared to genotype-specific DL^s varies according to the specific set of genotypes used and the environment in which they are tested. For instance, the early and late percentile-maturity groups differed from the 50th-percentile reference by as little as no difference to as much as 1.4 h and 2.4 h, respectively (Supplementary File S3). The larger differences occurred at higher latitudes where daily rates of photoperiodic change were greatest. As expected, this difference reduced to zero as a function of decreasing rates in photoperiodic change (Fig. 2d).

Using METs for modeling the PRN-FTP

To test approaches for modeling the PRN-FTP from METs, we combined flowering time data from multiple projects totaling 37 field experiments (dataset D4) that included, albeit with imbalanced data (Supplementary Table S1), a common set of seven genotypes of tropical origin that were expected to be photoperiod sensitive. This was used to compare procedures for estimating genotype-specific PRN-FTP parameters for flowering time *per se* (intercept), critical photoperiod (threshold), and photoperiod sensitivity (slope) using a two-phase regression model (see Methods; Fig. 3).

Using MET data to construct the PRN-FTP makes the simplistic assumption that physiological sensitivities to temperature and photoperiod are the only environmental factors influencing flowering time. Although these are dominant factors, other variables can also affect maize growth and development, but the specific causes are often unknown and likely to vary from one field environment to another. Therefore, we devised an approach to control for latent effects on flowering time and evaluated how adjusted values for T_t^{em-ant} impact PRN-FTP parameter estimation. Using

a designated set of photoperiod-insensitive control genotypes present in the D4 MET, their overall mean T_t^{em-ant} across environments was defined as an expected value for the specific effect of temperature on flowering time (i.e. for photoperiod insensitive genotypes, T_t^{em-ant} is expected to be the same across environments, with deviations attributed to latent variables; see Materials and methods). Then, environment-specific deviations from the overall mean were used to adjust the T_t^{em-ant} values for the remaining genotypes in each of the corresponding environments. Figure 3 portrays this procedure for one genotype and how it can affect estimates of the PRN-FTP parameters.

When tested using genotype-specific DL^s values for each of the seven tropical genotypes, latent variable adjustment of T_t^{em-ant} enhanced the precision of the overall model fit of the PRN-FTP by an average of 2-fold (Table 2). Using adjusted values also led to changes in the estimated thresholds of sensitivity, which in turn resulted in differences in the estimated flowering times *per se* by as much as 5% and slopes of sensitivity by as much as 77% (Table 2).

As described in the previous section, genotypes with a different BVP can experience different photoperiods within environments, such that points along the DL^s -environmental axis of the PRN-FTP may differ among genotypes in a common MET. This caused us to question the standard approach to modeling reaction norms from METs where all genotypes are assumed to experience the same environmental conditions in each field (i.e. values for a given environmental covariate is assumed to be common for all genotypes). If the specific conditions experienced by different genotypes are sufficiently large, this could impact parameter estimates of a reaction norm. To test this, we compared modeling the PRN-FTP using DL^s obtained from the BVP for each genotype vs the 50th-percentile BVP as a common reference. The seven genotypes presented adequate variation for testing this: compared to the 50th-percentile reference point, genotype-specific values for the BVP ranged from 266°Cd to 399°Cd, corresponding to the 16th and 89th percentiles of the BVP distribution estimated from 284 genotypes (Table 1). However, the set of environments in the MET network of dataset D4 presented smaller contrasts in DL^s than would occur at higher latitude (European) environments (Fig. 2b): the largest difference in DL^s between these specific genotypes and the common reference was 0.2 h. In this case, changes in

Table 2. Impact of latent variable adjustment on PRN-FTP parameter estimation for different maize genotypes.

Genotype	Intercept ($^{\circ}\text{Cd}$)	Threshold (h)	Slope ($^{\circ}\text{Cd h}^{-1}$)	RMSE ^a
Unadjusted values with genotype-specific DL^s				
CML10	851.0 \pm 28.6	12.3 \pm 0.6	44.3 \pm 9.7	82.0
CML258	934.6 \pm 33.4	12.3 \pm 0.7	42.1 \pm 11.4	95.4
CML277	856.5 \pm 22.1	14.5 \pm 0.6	96.7 \pm 18.7	76.0
CML341	802.0 \pm 24.7	12.3 \pm 0.6	49.1 \pm 8.4	71.2
CML373	815.2 \pm 30.6	12.3 \pm 1.1	35.9 \pm 10.7	67.5
Tzi8	858.0 \pm 29.1	12.4 \pm 1.1	30.9 \pm 9.9	86.4
Tzi9	809.0 \pm 29.5	12.2 \pm 1.1	26.3 \pm 9.3	85.0
Adjusted values with genotype-specific DL^s				
CML10	872.8 \pm 16.7	12.3 \pm 0.6	36.9 \pm 5.6	47.7
CML258	953.8 \pm 21.2	12.3 \pm 0.9	37.7 \pm 7.2	60.5
CML277	869.8 \pm 9.2	14.5 \pm 0.6	87.7 \pm 8.0	31.3
CML341	846.0 \pm 9.8	14.3 \pm 0.6	86.7 \pm 7.9	33.8
CML373	853.1 \pm 11.6	12.3 \pm 0.8	26.4 \pm 4.0	25.6
Tzi8	888.8 \pm 14.7	14.3 \pm 1.0	44.3 \pm 10.7	52.8
Tzi9	842.1 \pm 11.2	14.4 \pm 0.9	41.8 \pm 8.8	40.0
Adjusted values with common reference DL^s				
CML10	873.7 \pm 16.5	12.3 \pm 0.6	37.5 \pm 5.7	47.6
CML258	955.8 \pm 21.0	12.3 \pm 0.9	37.7 \pm 7.3	60.5
CML277	870.2 \pm 9.3	14.3 \pm 0.5	77.0 \pm 7.1	32.1
CML341	846.9 \pm 9.9	14.3 \pm 0.6	83.2 \pm 7.6	34.2
CML373	853.5 \pm 11.5	12.2 \pm 0.8	26.3 \pm 4.0	25.5
Tzi8	888.6 \pm 14.7	14.5 \pm 1.1	47.9 \pm 11.6	52.8
Tzi9	841.9 \pm 11.2	14.5 \pm 0.8	43.2 \pm 9.0	39.9

^a Root mean squared error (RMSE) is reported for the full bilinear model.

coefficient estimates for thresholds of sensitivity and flowering time *per se* were negligible, but the slope parameter for photoperiod sensitivity changed by 12% for one of the genotypes (Table 2). Nevertheless, these results show that intraenvironment variation in DL^s among genotypes can affect PRN-FTP parameters estimated from MET data. Even for this small sample of genotypes, Fig. 4 highlights a wide range of diversity for flowering time plasticity in maize consisting of unique parameterizations of the PRN-FTP.

Relating components of the PRN-FTP to understand maize adaptation

Since flowering time *per se* and photoperiod sensitivity underlie flowering time adaptation across environments (Choquette et al. 2023), we questioned how the trait space of these PRN-FTP parameters is structured among primary breeding pools of maize. For this, we assembled a MET dataset (D5) from 19 field trials with a common set of genotypes consisting of tropical, temperate, and admixed breeding material. Computational envirotyping showed that DL^s for the D5 MET was restricted to two small intervals of photoperiod conditions, with three environments of 11.9 to 12.4 h photoperiod and 16 environments of 14.5 to 16.5 h photoperiod. With this density of data and gap in coverage of DL^s , the bilinear function for the PRN-FTP could not be reliably fit. Besides, the collection of material included photoperiod insensitive genotypes that do not follow a bilinear response to photoperiod. In this case, the PRN-FTP was modeled using an LD–SD method based on linear regression after, as previously described, adjusting for latent variables with a designated set of control genotypes. Examining the relationship between flowering time *per se* and photoperiod sensitivity showed that temperate and tropical material occupy distinct territories of the trait space (Fig. 5; Supplementary File S6). Temperate genotypes tend to have a lower flowering time *per se* and nearly no photoperiod sensitivity, while tropical genotypes tend to have a higher flowering time *per se* coupled with a large range in photoperiod sensitivity. Fitting genetic expectations for polygenic traits, genotypes with

admixed ancestry are positioned between these two regions of the trait space.

Discussion

Understanding trait plasticity is important for adapting crops to new environments. To study the variation in plastic responses, METs allow large collections of genotypes to be characterized across environmental gradients. When modeling genotype–environment effects, the assumption—implicit in standard models—is that all genotypes experience the same conditions in each environment (an exception: Millet et al. 2019). However, as demonstrated in this study, due to phenological variation and stage-specific sensitivities, different genotypes within each field environment may not experience identical environmental conditions. This can complicate the definition of environmental indices for modeling reaction norms from METs, challenging standard analyses that assume common environmental conditions are sensed by all genotypes. Based on the ecophysiology of maize flowering time, the current study defines a new metric, DL^s , for quantifying the specific photoperiods sensed by different genotypes within and across environments. Using DL^s to envirotype maize fields in the Northern Hemisphere, we showed that, at high latitudes, where cooler temperatures that slow development combine with relatively large daily rates of photoperiodic change, genotypes in the same environment can experience more than a 1 h difference in DL^s (Fig. 2). This occurs more often and is more pronounced across maize environments in Europe than in the USA due to higher rates of daily photoperiodic change (Fig. 2d). Thus, to provide more accurate information about the variation in trait plasticity, the construction of genotype-specific reaction norms for flowering time and other traits should be considered on a case-by-case basis.

Constructing the PRN-FTP from METs is the most practical approach for studying the diversity of flowering time plasticity, but this is challenged by the geographical structure of photoperiod (Fig. 2) and the sensitivity of parameter estimation to gaps in DL^s (Table 2, Fig. 4). Testing across numerous field sites spanning nearly an entire hemisphere is required to capture a sufficient range and density of DL^s to model genotypic variation in the PRN-FTP. We found that currently available MET datasets for maize do span LD and SD conditions but have limited to no coverage of DL^s from 12.4 to 14.5 h, part of the range for expected variation in the critical photoperiod for maize (Rood and Major 1980; Kiniry et al. 1983a). With scant information on critical photoperiods for maize, and given the dependence of accurate threshold estimation for regression analysis of the PRN-FTP (Table 2), envirotyping with DL^s could be used to design new METs for future research on flowering time plasticity.

The PRN-FTP provides a parsimonious model for flowering time plasticity, taking into account the dominant effects of temperature and photoperiod. However, in METs, latent variables can affect flowering time, requiring appropriate adjustments. In particular, constructing the PRN-FTP from thermal time estimates can be obscured by the influence of other factors besides temperature on growth and development, such as drought (Herrero and Johnson 1981; Harrison et al. 2014). To address this issue, we applied a between-environment covariate adjustment using photoperiod-insensitive control genotypes expected to have the same thermal time to anthesis across LD and SD environments. This consistently resulted in a more precise fit of the bilinear response function for the PRN-FTP (Table 2; Fig. 3). Nevertheless, it is important to acknowledge that the choice of a

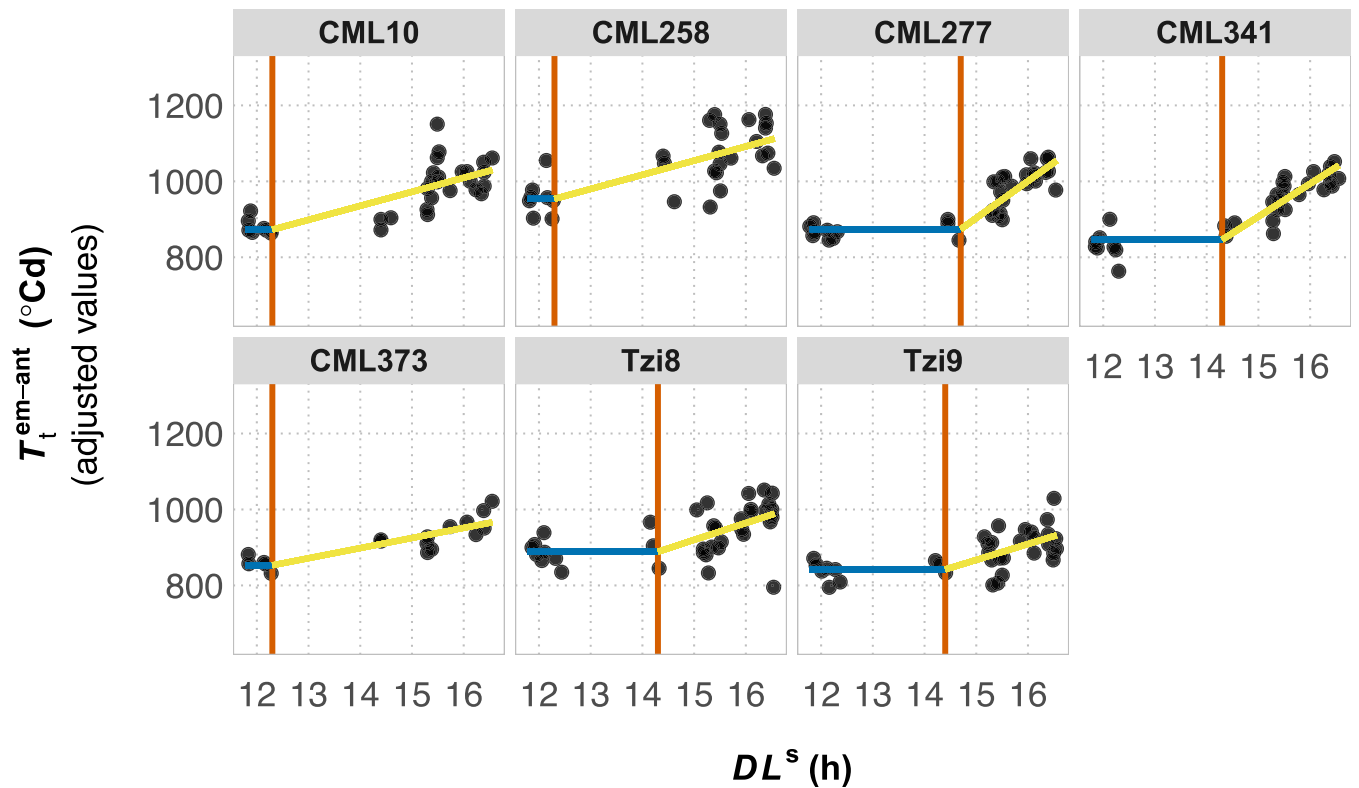


Fig. 4. The PRN-FTP for seven tropical genotypes of maize. For each genotype, the plots show the three PRN-FTP parameters estimated from the bilinear function fitted using latent-variable adjusted BLUEs for thermal time from crop emergence to anthesis ($T_t^{\text{em-ant}}$) in relation to sensed daylength (DL^s). Parameter estimates are shown for the flowering time *per se* (blue line), the critical threshold value (red line), and the photoperiod sensitivity (yellow line).

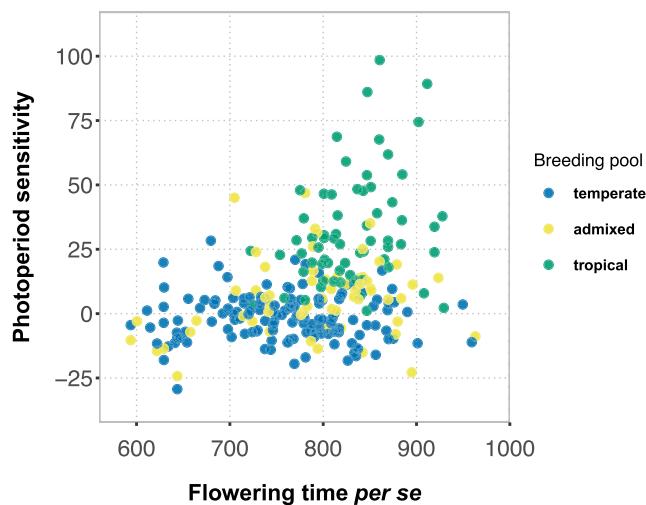


Fig. 5. The trait space for flowering time *per se* and photoperiod sensitivity in maize breeding material. Points correspond to genotypic values for flowering time *per se* ($^{\circ}\text{Cd}$) and photoperiod sensitivity ($^{\circ}\text{Cd h}^{-1}$), estimated using the LD-SD regression method on latent-variable adjusted BLUEs. Breeding pools are represented by samples of genotypes previously assigned to temperate ($n = 109$), admixed ($n = 61$), and tropical ($n = 66$) sources based on structure analysis of marker data (Liu et al. 2003).

control group could introduce some bias, as it may uniquely vary in other ecophysiological responses. Another challenge in modeling the PRN-FTP is that not all genotypes exhibit a clear bilinear response. For example, photoperiod-insensitive genotypes only display differences in flowering time *per se*, rendering the bilinear regression function invalid. In such cases, linear regression using

the LD-SD method is the most appropriate way of capturing the relationship between $T_t^{\text{em-ant}}$ and DL^s . Thus, while the PRN-FTP offers a valuable framework for understanding flowering time plasticity, careful consideration of latent effects, choice of control group, and genotype-specific responses is necessary for accurate modeling. Future work could consider alternative statistics to simultaneously model mixtures of genotypes with bilinear and linear reaction norm structures for the PRN-FTP.

A large body of work has elucidated the GRN-topology of multiple pathways involved in the transduction of signals that control flowering time in plants (Srikanth and Schmid 2011). Reflective of this complex regulatory system, MET mapping studies have shown the genetic architecture of phenotypic variation in days to flowering to be polygenic (e.g. maize—Buckler et al. 2009). While many genes are involved, using ecophysiology to redefine the context for genetic mapping can clarify the roles of individual loci or genes in relation to the GRN. As one example from maize, mapping variation in the difference between thermal time to flowering in LD and SD environments—an ecophysiological transformation of days to flowering into a measure of photoperiod sensitivity—led to the identification of a causal variant affecting the regulation of the photoperiod sensitivity pathway (Hung et al. 2012; Yang et al. 2013). The same study by Hung et al. (2012) demonstrated that this approach isolates loci specifically responsive to photoperiod from other loci that contribute to variation in flowering time in other ways. Nevertheless, the full topology and context-dependent expression of the GRN regulating flowering time remains unresolved, let alone its connections across physiological to whole-plant scales. We expect that using DL^s -guided MET design to estimate and decompose variation in flowering time *per se*, critical photoperiods, and photoperiod sensitivity

will help to further disentangle the genetic architectures of these context-specific traits. By relating these architectures to the GRN, this approach will facilitate testing of hypotheses on the multiscale relationships and genotype–environment interactions for flowering time.

Flowering time adaptations have facilitated the evolution and geographical spread of plant species (Gaudinier and Blackman 2019). The expansion of maize from its tropical origins to shorter growing seasons in the temperate zone was mediated by selection for early flowering time (Vigouroux *et al.* 2008; Tenailon and Charcosset 2011; Swarts *et al.* 2017), with evidence of selection on multiple pathways of the GRN (Brandenburg *et al.* 2017). Distinct breeding material was established from locally preadapted populations that have largely persisted as separate pools of tropical and temperate maize (Liu *et al.* 2003). Taken together, we reasoned that the PRN-FTP trait space of flowering time *per se* and photoperiod sensitivity for modern varieties representing these pools would reflect the historical perspective of adaptation and subsequent breeding in maize. Figure 5 corroborates this: assuming tropical genotypes reflect an ancestral state defined by moderate to late flowering time *per se* (adaptation to the long, warm growing seasons in the tropics) and segregation for photoperiod sensitivity (weak to no selection in SD environments), temperate maize shows both reduced flowering time *per se* and photoperiod sensitivity (adaptations for a shortened crop cycle). While this general structuring of plasticity between tropical and temperate breeding pools could be expected, Fig. 5 reveals an empty territory of the space where essentially no genotypes exist that are both early *per se* and sensitive to photoperiod. Nevertheless, this combination would also condition a maturity time adapted to many temperate environments. We hypothesize that this is a byproduct of the preadaptation history and subsequent breeding of maize, and not indicative of an intrinsic coupling between different pathways of the GRN or physiological controls of flowering time. This is supported by results from experimental evolution for early flowering time in tropical populations under contrasting photoperiod conditions. In LD environments, photoperiod sensitivity and flowering time *per se* are coselected but show different rates of change across generations, with photoperiod sensitivity rapidly eliminated (Teixeira *et al.* 2015; Choquette *et al.* 2023). In contrast, in SD environments, responses to selection can be attributed to flowering time *per se* with no changes observed for photoperiod sensitivity. This highlights how the PRN-FTP can be used for studying crop diversity, and that knowledge about the historical context of adaptation and breeding can aid in interpreting the observed patterns in the PRN-FTP-derived trait space.

Conclusions

In this study, we explored various aspects of a physiological reaction norm for modeling flowering time plasticity in maize. Envirotyping with DL^s is a valuable tool for examining the global distribution of photoperiodic sensing in maize and constructing the PRN-FTP from MET data. Notably, the geographical distribution of current public MET networks for maize are concentrated in LD and SD environments with discontinuity in DL^s across the critical photoperiod range. This hinders investigation of the PRN-FTP for maize and accurate modeling of flowering time $G \times E$, warranting further experimentation. The DL^s index can be used for the design of new MET networks to address this.

The PRN-FTP model provides an ecophysiological framework for decomposing and understanding phenotypic variation in

flowering time measured in days. For a specific genotype, the pace of development towards reproductive transition is affected by temperature fluctuations within an environment, with the magnitude of this influence varying across environments based on the unique temperature patterns. When contrasting genotypes are present in the same environments, interactions between temperatures and genetic variation in rates of development (phyllochron) and durations of reproductive transition (BVP) gives rise to variation in the timing of photoperiod sensitization. In turn, genetic variation in critical thresholds and photoperiod sensitivities lead to secondary interactions with daily rates of photoperiodic change and exposure to further temperature fluctuations within and across environments. This highlights the interplay between genetic and environment effects that shape phenotypic variation in flowering time.

Lastly, as the PRN-FTP model is based on common ecophysiological processes, we expect that it can be extended to other crops. Investigating the trait space of PRN-FTP components could provide valuable insights into flowering time adaptations across species. Our findings underscore the significance of considering the historical context of adaptation and breeding in unraveling the genetic and physiological underpinnings of complex traits. This, in turn, holds promising implications for future crop improvement endeavors.

Data availability

Data and metadata from this study are available in [Supplementary Files](#) at Dryad (<https://doi.org/10.5061/dryad.x95x69pth>). Sources of external data are indicated in the methods sections and [Supplementary Table S1](#) (also see Acknowledgments). Computer code for envirotyping DL^s and fitting the PRN-FTP is available at: <https://github.com/maizeatlas/prnftp>.

[Supplemental material](#) available at G3 online.

Acknowledgments

This study was made possible thanks to the production and availability of datasets from prior and ongoing projects: the EXPOSE and PhotoGrid projects at INRAE-LEPSE (ANR-16-IDEX-0006; France 2030 program; Post AgreenSkills Fund), the INVITE project (European Union's Horizon 2020 research and innovation program, grant no. 817970), the Maize ATLAS project (USDA-ARS, grant no. 2011-67003-30342), the Multiple Disease Resistance project (North Carolina State University, Cornell University, and University of Delaware collaboration), the Genomes-to-Fields Initiative (<https://www.genomes2fields.org/home/>), and the Panzea project (NSF-PGRP, grant no. 1238014). We wish to thank a number of people who contributed to this study: (i) Mainassara Abdou Zaman-Allah, Terence Molnar, and Prasanna Boddupalli from CIMMYT for providing much of the germplasm used for panel A; (ii) Alexis Bédie, Llorenç Cabrera-Bosquet, Nicole Choquette, Arnaud Desbiez-Piat, Thomas Laisné, Noé Lalouette-Marrier d'Unienville, Maëlle Lis, Anthony Rosello, Javier Soto Mendoza, and Benoît Suard for supporting the PhenoArch platform experiments at Montpellier, FR; (iii) Arnaud Brunet, Bernard Lagardere, and Jean-Rene Loustalot from the experimental station at Saint-Martin-de-Hinx, FR for supporting germplasm management and field testing; (iv) the ISRA team Ibrahima Sarr, Malick Ndiaye, Awa Mbengue, Abdoulaye Hoth, and Alain Audebert (CIRAD) for field trial data from Nioro du Rip, SN; and (v) the Moreno Retis team José Moreno and Luis Rodríguez for field trial data from Puerto Vallarta, MX.

Funding

This work was supported by the French National Research Agency (ANR-16-IDEX-0006 and ANR-24-CE45-3875-01), the France 2030 program, project EXPOSE (PAF_18) supported by INRAE, and the European Union's Horizon 2020 research and innovation program, grant no. 817970.

Conflicts of interest

The authors declare that the research was conducted in the absence of any commercial or financial relationships that could be construed as a potential conflict of interest.

Author contributions

JD and RJW: conceptualization; CP, CW, and RJW: resources; JD, CP, KJ, EM, and RJW: investigation; JD, CP, JR, and RJW: data curation; JD, PM, BP, and RJW: methodology; JD, JR, KJ, and RJW: formal analysis; JD and RJW: writing—original draft; EM, JR, PM, and KJ: writing—review & editing; BP, CW, and RJW: supervision; EM and RJW: funding acquisition.

Literature cited

- Andrieu B, Hillier J, Birch C. 2006. Onset of sheath extension and duration of lamina extension are major determinants of the response of maize lamina length to plant density. *Ann Bot.* 98(5): 1005–1016. <https://doi.org/10.1093/aob/mcl177>
- Bassiri A, Irish EE, Poethig RS. 1992. Heterochronic effects of Teopod 2 on the growth and photosensitivity of the maize shoot. *Plant Cell.* 4(4):497–504. <https://doi.org/10.2307/3869450>
- Bendix C, Mendoza JM, Stanley DN, Meeley R, Harmon FG. 2013. The circadian clock-associated gene *gigantea1* affects maize developmental transitions. *Plant Cell Environ.* 36(7):1379–1390. <https://doi.org/10.1111/pce.2013.36.issue-7>
- Blümel M, Dally N, Jung C. 2015. Flowering time regulation in crops—what did we learn from Arabidopsis? *Curr Opin Biotechnol.* 32: 121–129. <https://doi.org/10.1016/j.copbio.2014.11.023>
- Bonnett OT. 1954. The inflorescences of maize. *Science.* 120(3107): 77–87. <https://doi.org/10.1126/science.120.3107.77>
- Bradshaw AD. 1965. Evolutionary significance of phenotypic plasticity in plants. *Adv Genet.* 13:115–155. [https://doi.org/10.1016/S0065-2660\(08\)60048-6](https://doi.org/10.1016/S0065-2660(08)60048-6)
- Brandenburg JT, Mary-Huard T, Rigauil G, Hearne SJ, Corti H, Joets J, Vitte C, Charcosset A, Nicolas SD, Tenaillon MI. 2017. Independent introductions and admixtures have contributed to adaptation of European maize and its American counterparts. *PLoS Genet.* 13(3):e1006666. <https://doi.org/10.1371/journal.pgen.1006666>
- Buckler ES, Holland JB, Bradbury PJ, Acharya CB, Brown PJ, Browne C, Ersoz E, Flint-Garcia S, Garcia A, Glaubitz JC, et al. 2009. The genetic architecture of maize flowering time. *Science.* 325(5941): 714–718. <https://doi.org/10.1126/science.1174276>
- Buckley LB, Briones Ortiz BA, Caruso I, John A, Levy O, Meyer AV, Riddell EA, Sakairi Y, Simonis JL. 2023. TrenchR: an R package for modular and accessible microclimate and biophysical ecology. *PLOS Clim.* 2(8):e0000139. <https://doi.org/10.1371/journal.pclm.0000139>
- Cabrera-Bosquet L, Fournier C, Brichet N, Welcker C, Suard B, Tardieu F. 2016. High-throughput estimation of incident light, light interception and radiation-use efficiency of thousands of plants in a phenotyping platform. *New Phytol.* 212(1):269–281. <https://doi.org/10.1111/nph.2016.212.issue-1>
- Choquette NE, Holland JB, Weldekidan T, Drouault J, de Leon N, Flint-Garcia S, Lauter N, Murray SC, Xu W, Wissner RJ. 2023. Environment-specific selection alters flowering-time plasticity and results in pervasive pleiotropic responses in maize. *New Phytol.* 238(2):737–749. <https://doi.org/10.1111/nph.v238.2>
- Colasanti J, Coneva V. 2009. Mechanisms of floral induction in grasses: something borrowed, something new. *Plant Physiol.* 149(1):56–62. <https://doi.org/10.1104/pp.108.130500>
- Coles ND, McMullen MD, Balint-Kurti PJ, Pratt RC, Holland JB. 2010. Genetic control of photoperiod sensitivity in maize revealed by joint multiple population analysis. *Genetics.* 184(3):799–812. <https://doi.org/10.1534/genetics.109.110304>
- Cooper M, Tang T, Cho C, Hart T, Hammer G, Messina C. 2020. Integrating genetic gain and gap analysis to predict improvements in crop productivity. *Crop Sci.* 60(2):582–604. <https://doi.org/10.1002/csc2.v60.2>
- Dong Z, Danilevskaya O, Abadie T, Messina C, Coles N, Cooper M. 2012. A gene regulatory network model for floral transition of the shoot apex in maize and its dynamic modeling. *PLoS One.* 7(8):e43450. <https://doi.org/10.1371/journal.pone.0043450>
- Ducrocq S, Madur D, Veyrieras JB, Camus-Kulandaivelu L, Kloiber-Maitz M, Prestler T, Ouzunova M, Manicacci D, Charcosset A. 2008. Key impact of *Vgt1* on flowering time adaptation in maize: evidence from association mapping and ecogeographical information. *Genetics.* 178(4):2433–2437. <https://doi.org/10.1534/genetics.107.084830>
- Finlay KW, Wilkinson GN. 1963. The analysis of adaptation in a plant-breeding programme. *Aust J Agric Res.* 14(6):742–754. <https://doi.org/10.1071/AR9630742>
- Flint-Garcia SA, Thuillet AC, Yu J, Pressoir G, Romero SM, Mitchell SE, Doebley J, Kresovich S, Goodman MM, Buckler ES. 2005. Maize association population: a high-resolution platform for quantitative trait locus dissection. *Plant J.* 44(6):1054–1064. <https://doi.org/10.1111/tj.2005.44.issue-6>
- Fong Y, Chongzhi D, Huang Y, Gilbert PB. 2017a. Model-robust inference for continuous threshold regression models. *Biometrics.* 73(2):452–462. <https://doi.org/10.1111/biom.12623>
- Fong Y, Huang Y, Gilbert PB, Permar SR. 2017b. chngpt: threshold regression model estimation and inference. *BMC Bioinformatics.* 18(1):1–7. <https://doi.org/10.1186/s12859-017-1863-x>
- Forsythe WC, Rykiel EJ, Stahl RS, Wu H, Schoolfield RM. 1995. A model comparison for daylength as a function of latitude and day of year. *Ecol Modell.* 80(1):87–95. [https://doi.org/10.1016/0304-3800\(94\)00034-F](https://doi.org/10.1016/0304-3800(94)00034-F)
- Gaudinier A, Blackman BK. 2019. Evolutionary processes from the perspective of flowering time diversity. *New Phytol.* 225(5): 1883–1898. <https://doi.org/10.1111/nph.v225.5>
- Guo L, Wang X, Zhao M, Huang C, Li C, Li D, Yang CJ, York AM, Xue W, Xu G, et al. 2018. Stepwise cis-regulatory changes in *ZCN8* contribute to maize flowering-time adaptation. *Curr Biol.* 28(18):3005–3015.e4 <https://doi.org/10.1016/j.cub.2018.07.029>
- Guo T, Wei J, Li X, Yu J. 2023. Environmental context of phenotypic plasticity in flowering time in sorghum and rice. *J Exp Bot.* 75(3): 1004–1015. <https://doi.org/10.1093/jxb/erad398>
- Harrison MT, Tardieu F, Dong Z, Messina CD, Hammer GL. 2014. Characterizing drought stress and trait influence on maize yield under current and future conditions. *Glob Chang Biol.* 20(3): 867–878. <https://doi.org/10.1111/gcb.2014.20.issue-3>
- Herrero MP, Johnson RR. 1981. Drought stress and its effects on maize reproductive systems. *Crop Sci.* 21(1):105–110. <https://doi.org/10.2135/cropsci1981.0011183X002100010029x>

- Hung HY, Shannon LM, Tian F, Bradbury PJ, Chen C, Flint-Garcia SA, McMullen MD, Ware D, Buckler ES, Doebley JF, et al. 2012. ZmCCT and the genetic basis of day-length adaptation underlying the postdomestication spread of maize. *Proc Natl Acad Sci U S A*. 109(28):E1913–E1921. <https://doi.org/10.1073/pnas.1203189109>
- Itoh H, Nonoue Y, Yano M, Izawa T. 2010. A pair of floral regulators sets critical day length for *Hd3a* florigen expression in rice. *Nat Genet*. 42(7):635–638. <https://doi.org/10.1038/ng.606>
- Jarquín D, Crossa J, Lacaze X, Du Cheyron P, Daucourt J, Lorgeou J, Piraux F, Guerreiro L, Pérez P, Calus M, et al. 2014. A reaction norm model for genomic selection using high-dimensional genomic and environmental data. *Theor Appl Genet*. 127(3): 595–607. <https://doi.org/10.1007/s00122-013-2243-1>
- Kiniry J, Ritchie JT, Musser RL. 1983a. Dynamic nature of the photoperiod response in maize. *Agron J*. 75:700–703. <https://doi.org/10.2134/agronj1983.00021962007500040029x>
- Kiniry J, Ritchie JT, Musser RL, Flint EP, Iwig WC. 1983b. The photoperiod sensitive interval in maize. *Agron J*. 75(4):687–690. <https://doi.org/10.2134/agronj1983.00021962007500040026x>
- Kiniry JR. 1991. Maize phasic development. In: Hanks J, Ritchie JT, editors. Modeling plant and soil systems. Agronomy Monographs Series. American Society of Agronomy, Inc., Crop Science Society of America, Inc., Soil Science Society of America, Inc. p. 55–70. <https://doi.org/10.2134/agronmonogr31.c4>
- Kusmec A, Srinivasan S, Nettleton D, Schnable PS. 2017. Distinct genetic architectures for phenotype means and plasticities in *Zea mays*. *Nat Plants*. 3(9):715–723. <https://doi.org/10.1038/s41477-017-0007-7>
- Lee SH, Choi CW, Park KM, Jung WH, Chun HJ, Baek D, Cho HM, Jin BJ, Park MS, No DH, et al. 2021. Diversification in functions and expressions of soybean *FLOWERING LOCUS T* genes fine-tunes seasonal flowering. *Front Plant Sci*. 12:1–16.
- Lejeune P, Bernier G. 1996. Effect of environment on the early steps of ear initiation in maize (*Zea mays* L.). *Plant Cell Environ*. 19(2): 217–224. <https://doi.org/10.1111/pce.1996.19.issue-2>
- Liu K, Goodman M, Muse S, Smith JS, Buckler E, Doebley J. 2003. Genetic structure and diversity among maize inbred lines as inferred from DNA microsatellites. *Genetics*. 165(4):2117–2128. <https://doi.org/10.1093/genetics/165.4.2117>
- Matsubara K, Yamanouchi U, Wang ZX, Minobe Y, Izawa T, Yano M. 2008. *Ehd2*, a rice ortholog of the maize *INDETERMINATE1* gene, promotes flowering by up-regulating *Ehd1*. *Plant Physiol*. 148(3): 1425–1435. <https://doi.org/10.1104/pp.108.125542>
- McFarland BA, Alkhalifah N, Bohn M, Hubert J, Buckler ES, Ciampitti I, Edwards J, Ertl D, Gage JL, Falcon CM, et al. 2020. Maize genomes to fields (G2F): 2014–2017 field seasons: genotype, phenotype, climatic, soil, and inbred ear image datasets. *BMC Res Notes*. 13(1): 4–9. <https://doi.org/10.1186/s13104-020-4922-8>
- Meng X, Muszynski MG, Danilevskaya ON. 2011. The FT-like ZCN8 gene functions as a floral activator and is involved in photoperiod sensitivity in maize. *Plant Cell*. 23(3):942–960. <https://doi.org/10.1105/tpc.110.081406>
- Millet EJ, Kruijer W, Coupel-Ledru A, Alvarez Prado S, Cabrera-Bosquet L, Lacube S, Charcosset A, Welcker C, van Eeuwijk F, Tardieu F. 2019. Genomic prediction of maize yield across European environmental conditions. *Nat Genet*. 51(6): 952–956. <https://doi.org/10.1038/s41588-019-0414-y>
- Minow MA, Ávila LM, Turner K, Ponzoni E, Mascheretti I, Dussault FM, Lukens L, Rossi V, Colasanti J. 2018. Distinct gene networks modulate floral induction of autonomous maize and photoperiod-dependent teosinte. *J Exp Bot*. 69(12):2937–2952. <https://doi.org/10.1093/jxb/ery110>
- Muller B, Martre P. 2019. Plant and crop simulation models: powerful tools to link physiology, genetics, and phenomics. *J Exp Bot*. 70(9): 2339–2344. <https://doi.org/10.1093/jxb/erz175>
- Nemoto Y, Nonoue Y, Yano M, Izawa T. 2016. *Hd1*, a CONSTANS ortholog in rice, functions as an *Ehd1* repressor through interaction with monocot-specific CCT-domain protein *Ghd7*. *Plant J*. 86(3):221–233. <https://doi.org/10.1111/tpj.2016.86.issue-3>
- Padilla JM, Otegui ME. 2005. Co-ordination between leaf initiation and leaf appearance in field-grown maize (*Zea mays*): genotypic differences in response of rates to temperature. *Ann Bot*. 96(6): 997–1007. <https://doi.org/10.1093/aob/mci251>
- Parent B, Tardieu F. 2012. Temperature responses of developmental processes have not been affected by breeding in different ecological areas for 17 crop species. *New Phytol*. 194(3):760–774. <https://doi.org/10.1111/nph.2012.194.issue-3>
- Parent B, Turc O, Gibon Y, Stitt M, Tardieu F. 2010. Modelling temperature-compensated physiological rates, based on the co-ordination of responses to temperature of developmental processes. *J Exp Bot*. 61(8):2057–2069. <https://doi.org/10.1093/jxb/erq003>
- Park SJ, Kim SL, Lee S, Je BI, Piao HL, Park SH, Kim CM, Ryu CH, Park SH, Xuan YH, et al. 2008. Rice *Indeterminate 1* (*OsId1*) is necessary for the expression of *Ehd1* (*Early heading date 1*) regardless of photoperiod. *Plant J*. 56(6):1018–1029. <https://doi.org/10.1111/j.1365-3113X.2008.03667.x>
- Rising J, Devineni N. 2020. Crop switching reduces agricultural losses from climate change in the United States by half under RCP 8.5. *Nat Commun*. 11(1):1–7. <https://doi.org/10.1038/s41467-020-18725-w>
- Rogers AR, Dunne JC, Romay C, Bohn M, Buckler ES, Ciampitti IA, Edwards J, Ertl D, Flint-Garcia S, Gore MA, et al. 2021. The importance of dominance and genotype-by-environment interactions on grain yield variation in a large-scale public cooperative maize experiment. G3 (Bethesda). 11(2):jkaa050. <https://doi.org/10.1093/g3journal/jkaa050>
- Rood SB, Major DJ. 1980. Responses of early corn inbreds to photoperiod. *Crop Sci*. 20(6):679–682. <https://doi.org/10.2135/cropsci1980.0011183X002000060001x>
- Roff DA. 1997. Evolutionary quantitative genetics. New York: Springer. <https://doi.org/10.1007/978-1-4615-4080-9>
- Sawa M, Kay SA. 2011. GIGANTEA directly activates *Flowering Locus T* in *Arabidopsis thaliana*. *Proc Natl Acad Sci U S A*. 108(28): 11698–11703. <https://doi.org/10.1073/pnas.1106771108>
- Sawa M, Nusinow DA, Steve KA, Imaizumi T. 2007. FKF1 and GIGANTEA complex formation is required for day-length measurement in *Arabidopsis*. *Science*. 318(5848):261–265. <https://doi.org/10.1126/science.1146994>
- Simpson GG, Dean C. 2002. *Arabidopsis*, the Rosetta stone of flowering time? *Science*. 296(5566):285–289. <https://doi.org/10.1126/science.296.5566.285>
- Sloat LL, Davis SJ, Gerber JS, Moore FC, Ray DK, West PC, Mueller ND. 2020. Climate adaptation by crop migration. *Nat Commun*. 11(1): 1–9. <https://doi.org/10.1038/s41467-020-15076-4>
- Song YH, Shim JS, Kinmonth-Schultz HA, Imaizumi T. 2015. Photoperiodic flowering: time measurement mechanisms in leaves. *Annu Rev Plant Biol*. 66(1):441–464. <https://doi.org/10.1146/arplant.2015.66.issue-1>
- Sparks A. 2018. nasapower: a NASA POWER global meteorology, surface solar energy and climatology data client for R. *J Open Source Softw*. 3(30):1035. <https://doi.org/10.21105/joss>
- Srikanth A, Schmid M. 2011. Regulation of flowering time: all roads lead to Rome. *Cell Mol Life Sci*. 68(12):2013–2037. <https://doi.org/10.1007/s00018-011-0673-y>

- Stephenson E, Estrada S, Meng X, Ourada J, Muszynski MG, Habben JE, Danilevskaya ON. 2019. Over-expression of the photoperiod response regulator *ZmCCT10* modifies plant architecture, flowering time and inflorescence morphology in maize. *PLoS One*. 14(2): e0203728. <https://doi.org/10.1371/journal.pone.0203728>
- Swarts K, Gutaker RM, Benz B, Blake M, Bukowski R, Holland J, Kruse-Peeples M, Lepak N, Prim L, Romay MC, et al. 2017. Genomic estimation of complex traits reveals ancient maize adaptation to temperate North America. *Science*. 357(6350): 512–515. <https://doi.org/10.1126/science.aam9425>
- Teixeira JE, Weldekidan T, De Leon N, Flint-Garcia S, Holland JB, Lauter N, Murray SC, Xu W, Hessel DA, Kleintop AE, et al. 2015. Hallauer's Tusón: a decade of selection for tropical-to-temperate phenological adaptation in maize. *Heredity* (Edinb). 114(2): 229–240. <https://doi.org/10.1038/hdy.2014.90>
- Tenaillon MI, Charcosset A. 2011. A European perspective on maize history. *C R Biol*. 334(3):221–228. <https://doi.org/10.1016/j.crvi.2010.12.015>
- van Voorn GA, Boer MP, Truong SH, Friedenberg NA, Gugushvili S, McCormick R, Bustos Korts D, Messina CD, van Eeuwijk FA. 2023. A conceptual framework for the dynamic modeling of time-resolved phenotypes for sets of genotype-environment-management combinations: a model library. *Front Plant Sci*. 14: 1–14. <https://doi.org/10.3389/fpls.2023.1172359>
- Vigouroux Y, Glaubitz JC, Matsuoka Y, Goodman MM, Sánchez GJ, Doebley J. 2008. Population structure and genetic diversity of New World maize races assessed by DNA microsatellites. *Am J Bot*. 95(10):1240–1253. <https://doi.org/10.3732/ajb.0800097>
- Wang E, Engel T. 1998. Simulation of phenological development of wheat crops. *Agric Syst*. 58(1):1–24. [https://doi.org/10.1016/S0308-521X\(98\)00028-6](https://doi.org/10.1016/S0308-521X(98)00028-6)
- Wang E, Martre P, Zhao Z, Ewert F, Maiorano A, Rötter RP, Kimball BA, Ottman MJ, Wall GW, White JW, et al. 2017. The uncertainty of crop yield projections is reduced by improved temperature response functions. *Nat Plants*. 3:1–11.
- Yang Q, Li Z, Li W, Ku L, Wang C, Ye J, Li K, Yang N, Li Y, Zhong T, et al. 2013. CACTA-like transposable element in *ZmCCT* attenuated photoperiod sensitivity and accelerated the postdomestication spread of maize. *Proc Natl Acad Sci U S A*. 110(42):16969–16974. <https://doi.org/10.1073/pnas.1310949110>
- Zabel F, Müller C, Elliott J, Minoli S, Jägermeyr J, Schneider JM, Franke JA, Moyer E, Dury M, Francois L, et al. 2021. Large potential for crop production adaptation depends on available future varieties. *Glob Chang Biol*. 27(16):3870–3882. <https://doi.org/10.1111/gcb.v27.16>
- Zhao Y, Zhao B, Xie Y, Jia H, Li Y, Xu M, Wu G, Ma X, Li Q, Hou M, et al. 2023. The evening complex promotes maize flowering and adaptation to temperate regions. *Plant Cell*. 35(1):369–389. <https://doi.org/10.1093/plcell/koac296>

Editor: D.-J. de Koning